HREM IMAGING OF SMALL Pt CLUSTERS DISPERSED IN Y-ZEOLITES

M. PAN, J.M. COWLEY and I.Y. CHAN *

Department of Physics, Arizona State University, Tempe, AZ 85287-1504, USA.
* *Chevron Research Company, P.O. Box 1627, Richmond, CA 94802-0627, U.S.A.*

Received 20 November 1989; accepted 21 February 1990

HREM, small Pt clusters, zeolites

High resolution electron microscopy (HREM) has been used to study dispersed Pt clusters in NaY- and USY-zeolites. All the samples contained 0.8% Pt and were reduced at temperatures of 300 °C, 500 °C and 650 °C. The size of the Pt clusters ranged from a few Å up to ~ 30 Å. When the incident electron beam was sufficiently strong, it caused some of the extremely small metal clusters to sinter. This was usually accompanied by zeolite damage. This in-situ sintering must be taken into consideration when interpreting the particle size distribution results obtained solely by TEM, especially for particles that are smaller than 10 Å. The minimum phase contrast imaging condition is demonstrated to be more appropriate than optimum defocus for detecting the extremely small Pt clusters inside the zeolite structures.

1. Introduction

The importance of zeolites as a catalytic material in petrochemical processing has been known for many years [1]. TEM has been shown to be very valuable in characterizing catalysts made up to zeolites containing dispersed metals [2,3]. The crystal structures of zeolites can be considered as framework aluminosilicates which are made up of a three-dimensional network of AlO_4 and SiO_4 tetrahedra linked to each other by sharing all of the oxygens [4]. The general formula of a zeolite for the crystallographic unit cell can be written as: $M_{x/n}[(AlO_2)_x(SiO_2)_y].wH_2O$, where M is the cation of valence n, w is the number of water molecules. Zeolite Y, along with X and faujasite, has a FCC lattice with an a_0 of about 24.74 Å. The unit cell contains 192 (Si, Al)O_4 tetrahedra. The structural units are the so-called β-cage and double 6-ring which are polyhedral arrangements of (Si, Al)O_4 tetrahedra. The structure can be simply visualized as a diamond structure with the replacement of each C atom by the β-cage which is tetrahedrally joined to other β-cages through the double 6-ring unit [4].

When catalytic metals are introduced into the zeolite matrix, it is important to determine the distribution of the metals. It would be especially informative if we can visualize small metallic clusters inside the open channels and the zeolite cages [5]. The orientational relationship, if any, between the metals and the zeolite structures would be an important clue to the catalytic behavior of a particular catalyst [6]. This presents a great challenge to the HREM technique because (1) the metal clusters of interest are very small (on the order of 10 Å or less), the strong phase contrast produced by the zeolite structure could easily obscure their contrast, and (2) the deterioration of the zeolite structure is rapid under HREM imaging conditions.

There are many studies on the crystal structures and defects of various zeolites by HREM [7–12]. However, the application of this technique has been limited mainly by the sensitivity of the nonconducting zeolites to electron beam damage [13,14]. Efforts have been made to develop methods for stabilizing the zeolite structures for TEM observations. Successful results have been achieved in some cases [15,16]. In this paper we will report some HREM studies of the small Pt clusters dispersed in the zeolite structures of 0.8% Pt/NaY and 0.8% Pt/USY catalysts.

2. Experimental

The catalysts were prepared by the incipient wetness impregnation of NaY zeolite with an aqueous solution of $Pt(NH_3)_4(NO_3)_2$ to provide 0.80 g Pt per 100 g zeolite. Each catalyst was dried overnight in a vacuum oven at 100 °C, heated at 5 °C per minute from room temperature to 150 °C in flowing dry air, heated at 5 °C per minute from 150 °C to 290 °C in a flowing mixture of 75% air and 25% steam, held at 290 °C in the flowing air stream mixture for two hours, and cooled to room temperature in dry air. The samples were then divided into three portions and reduced in H_2 at 1 atmosphere pressure. The ^{129}Xe NMR results and chemisorption results were presented in a previous publication [17]. The TEM samples were prepared by two methods, direct dispersion and ultramicrotomy. The zeolite powders were ground in an agate mortar and suspended in ethanol. After being further dispersed in the ultrasonic agitator, a drop of the suspension was put on a holey carbon grid and allowed to dry in air. This method for preparing catalyst TEM samples has been described by many authors [2,5,8].

All the HREM work was carried out in a JEOL JEM-200 CX with a top-entry stage and point resolution of 2.5 Å. The images were recorded at 200 kV and magnifications of either 100,000 or 130,000. The electron beam intensity was kept as low as possible with the selection of spot size 4 to minimize the beam damage to the zeolites. The samples were also examined at 400 kV with the JEOL JEM-4000EX but appeared to be more stable at 200 kV than 400 kV.

3. Results and discussions

3.1. Pt SIZE DISTRIBUTIONS IN NaY-ZEOLITES

The Pt dispersion in these samples had been studied using ^{129}Xe nuclear magnetic resonance spectroscopy (NMR) [17]. The results showed that when the samples were reduced at 300 °C and 500 °C, the average Pt cluster contained only ~ 6 and ~ 8 atoms respectively. After reduction at 650 °C, Pt migrated outside the β-cages and coalesced into larger clusters.

Our experimental observations, shown in fig. 1, are in qualitative agreement with these previous results. That is, the Pt cluster size at lower reduction temperatures is smaller than that at higher reduction temperatures. The HREM images in fig. 1 were recorded near optimum defocus so that the Pt particles could be identified as small black dots. After reduction at 300 °C almost no Pt clusters are visible in fig. 1a. As the reduction temperature increases, the number and size of the Pt clusters increase as seen in figs. 1b and 1c. The average particle size can be estimated from fig. 1 as ~ 10 Å for reduction at 500 °C and ~ 25 Å for reduction at 650 °C.

However, we have also observed the coalescence of small Pt particles under the electron beam irradiation and this certainly makes it difficult to obtain faithful size distributions for Pt particles in zeolites. The sintering process is shown in fig. 2 where the HREM images were recorded about 1 min apart in the sample of Pt/NaY reduced at 650 °C. In fig. 2, more and more black dots emerged with increasing exposure to the electron beam, suggesting that some of the Pt particles have sintered. From the ^{129}Xe NMR and chemisorption results [17], it was clear that the sample originally contained many extremely small Pt clusters which in general were not detectable in the initial HREM image. The "new" Pt particles were created from these originally invisible clusters. Figure 2 shows that sintering occurred at areas where the zeolites had already turned amorphous.

Figure 3 shows another example where the sintering process occurred in a region of high degree of crystallinity in Pt/NaY reduced at 500 °C. The time interval between the images was again about 1 min. In fig. 3a well-defined (111) lattice fringes from the zeolite along with some Pt clusters (10–20 Å) are clearly seen. Under electron beam irradiation, cross lattice fringes appeared along with more Pt clusters (figs. 3b and 3c). It was noticed that the cross fringes were not uniform and varied throughout the zeolite crystal. This suggests that the orientational change was on a local and the original zeolite fragment was made up of smaller grains. The electron beam caused the re-orientation of some grains with respect to others. This would have caused some rearrangement at the grain boundary.

It seems that local structure destruction of the zeolite support promoted the sintering of extremely small Pt clusters. The sintering process must involve first dislodging at least one Pt cluster from its anchored site in the zeolite, then

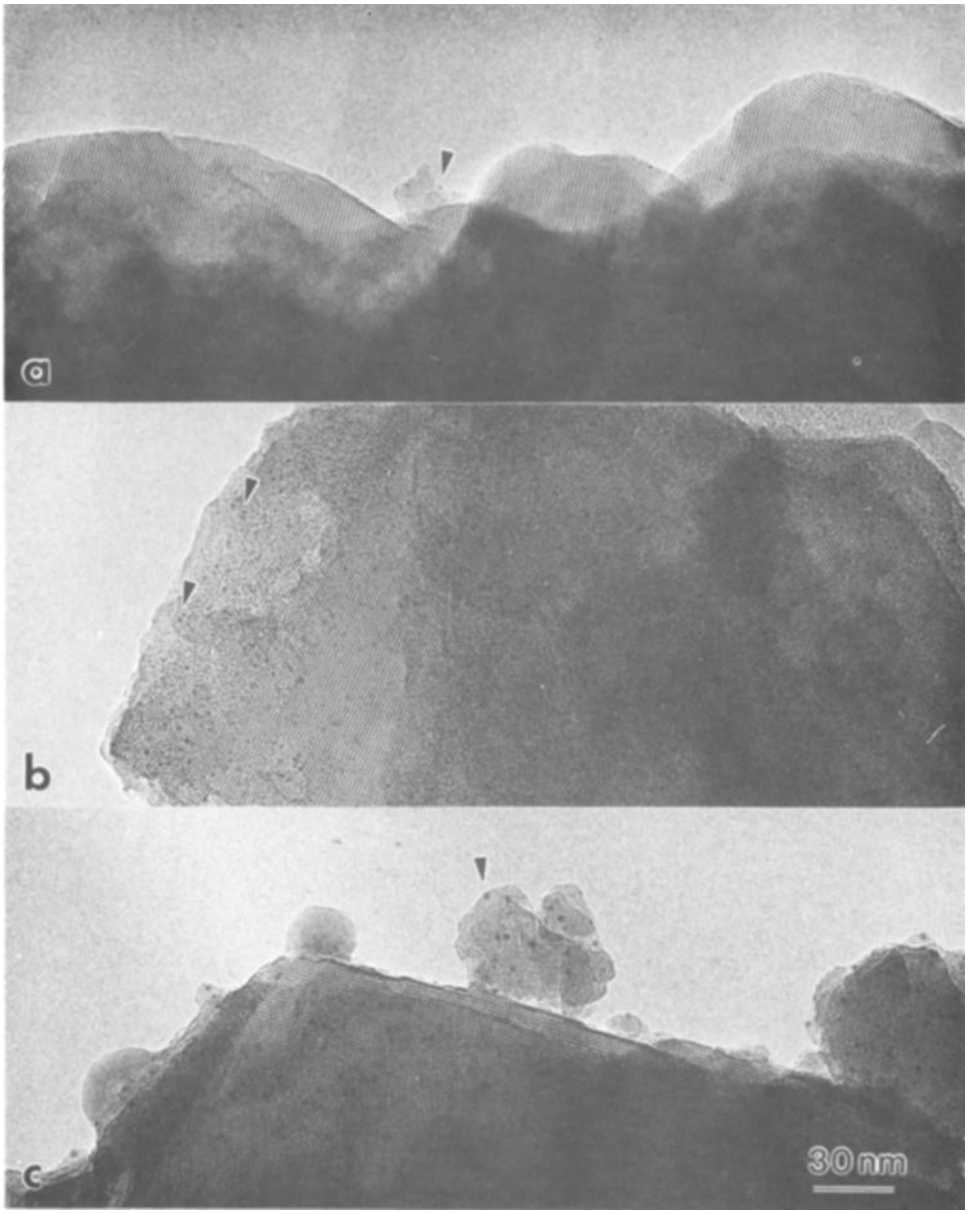

Fig. 1. HREM images of 0.8% Pt/ NaY reduced at (a) 300 ° C (b) 500 ° C (c) 650 ° C. Pt particle size increases with reduction temperature.

transport by diffusion to where it joins up with another Pt cluster. When the zeolite structure is damaged, the first step would be facilitated. Further growth of the Pt cluster would depend upon: (1) the zeolite damage rate, as the diffusion paths would be closed off when the zeolite turns amorphous, and (2) the electron

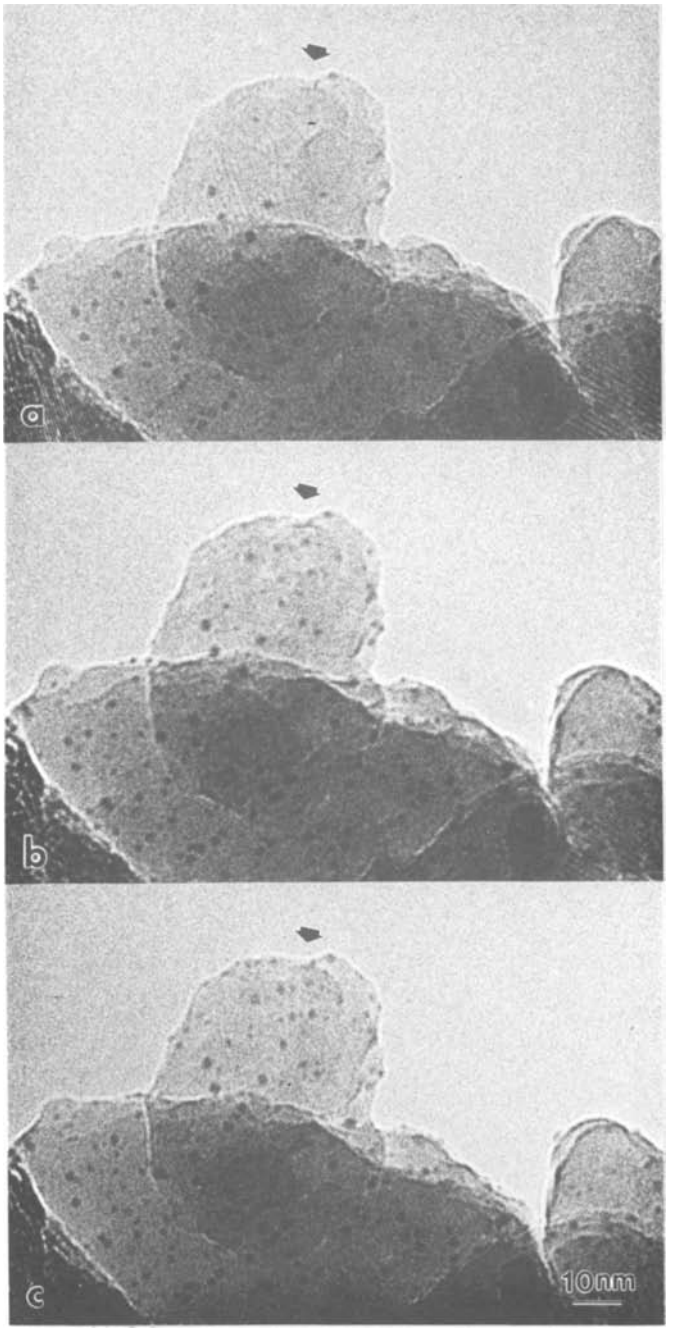

Fig. 2. Sequence of HREM images of Pt coalescence under electron beam irradiation in 0.8% Pt/NaY reduced at 650 °C. The images were recorded ~1 min apart. Arrows shows the region where the sintering occurred.

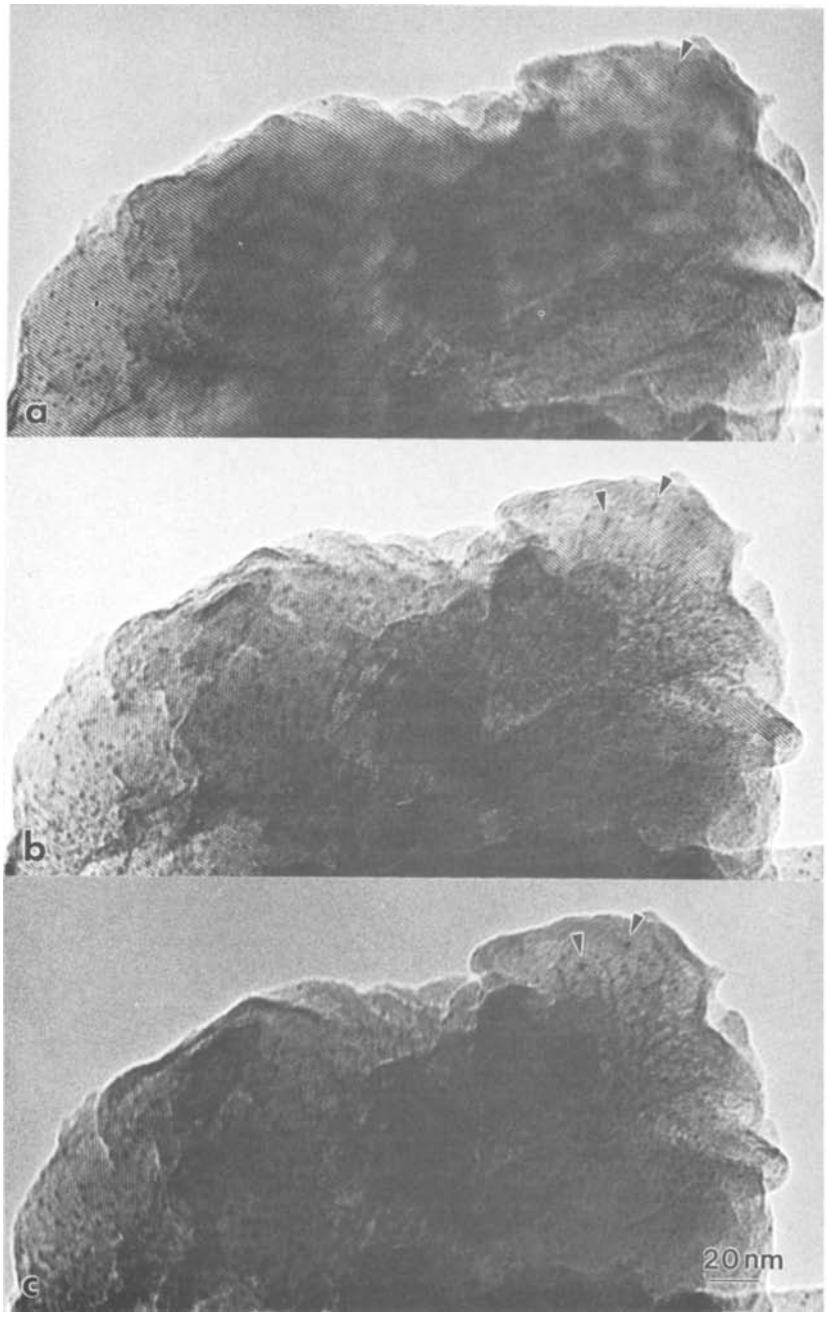

Fig. 3. Sequence of HREM images of the Pt coalescence under the incident electron beam in 0.8% Pt/NaY reduced at 500 °C. The time interval was ~1 min. The sintering of Pt particles was related to the structure rearrangement of the zeolite support.

beam intensity, as small metal particles could still be extremely mobile on amorphous support under the intense electron beam if it is not encased in the amorphous matrix. The fact that sintering occurred in both cases suggests that both the dislodging and the diffusion of the small Pt clusters are very fast processes. It was found that this in-situ sintering was observed more often in the NaY- than the USY-zeolites. This can be attributed to the greater structural stability of the USY-zeolites. In STEM where a much stronger beam is used, the sintering of Pt on both NaY and USY can be observed.

Our experimental results demonstrate that in general the particle size distributions of highly dispersed metals in zeolites determined solely by TEM are very sensitive to experimental conditions. This is especially true for zeolites that are easily damaged by the electron beam. Complementary techniques must be used in order to obtain any reliable and quantitative results.

3.2. IDENTIFICATION OF SMALL Pt CLUSTERS IN USY-ZEOLITES

For the samples prepared by microtoming, the detection of small metal particles becomes increasingly difficult when the particle size approaches that of the phase contrast structures of the support. It has been show [18] that the best imaging conditions are those that suppress the phase contrast from the support and emphasize the amplitude contrast from the particles. The detection of particles smaller than 10 Å generally requires sophisticated techniques in practice.

As seen in figs. 1b and 1c Pt clusters as small as 10 Å or less could be identified for Pt/NaY. For Pt in USY zeolites it was found that the detection of the same sized Pt clusters was more difficult. This difference in the visibility was related to the structural stability of the zeolite support under the electron beam. The higher damage rate of NaY resulted in a faster loss of its crystallinity. Therefore the phase contrast from NaY was weaker than that from USY. For this reason, it was harder to detect small Pt particles in Pt/USY than in Pt/NaY. We found that the minimum phase contrast imaging condition was more appropriate for detecting Pt clusters. Under this condition the small Pt particles appeared as small black dots on a low contrast background. Figure 4 compares HREM images of the same specimen area in [110] orientation recorded under (a) optimum defocus and (b) minimum phase contrast conditions. The sample is Pt/USY reduced at 500 °C. In the minimum phase contrast image many small black dots can be seen in the region where there was strong phase contrast from the zeolite at optimum defocus. These small black dots are believed to be the highly dispersed Pt particles. The thickness of the zeolite support is about 200 Å to 400 Å. The residual phase contrast from the support does not allow a clear definition of the particle edges.

To illustrate the image contrast difference of small metal particles in zeolite at different imaging conditions, image simulations have been carried out for Pt cluster of 55 atoms with a cuboctahedral shape in Y-zeolite in [110] projection.

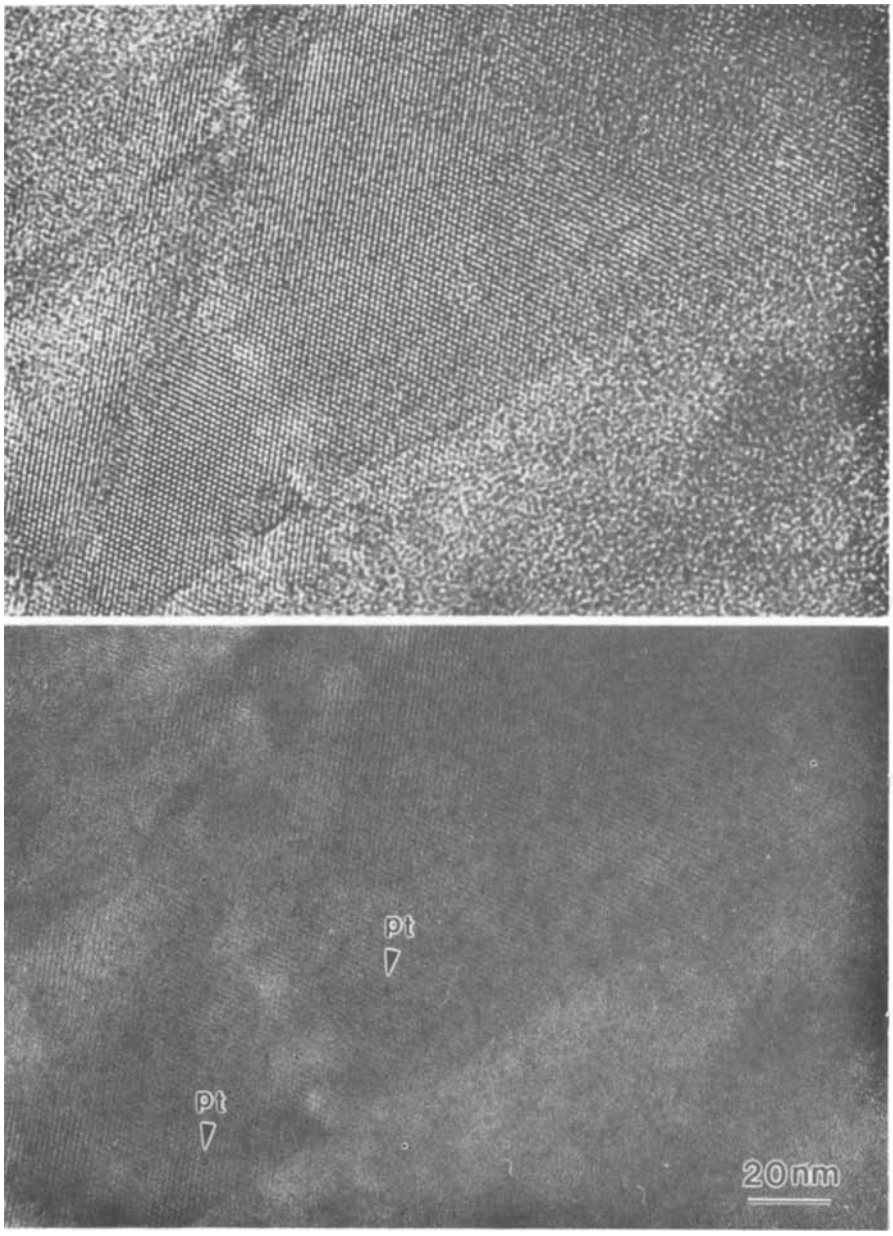

Fig. 4. HREM images of 0.8% Pt/USY reduced at 500 °C recorded from the same area at (a) optimum defocus and (b) minimum phase contrast conditions. The highly dispersed Pt particles can be identified in (b).

The simulation was intended for a JEOL JEM-200CX. The size of the Pt cluster was about 13 Å and the thickness of the zeolite support was chosen to be 35 Å. It should be pointed out that this particular example was not intended to match the

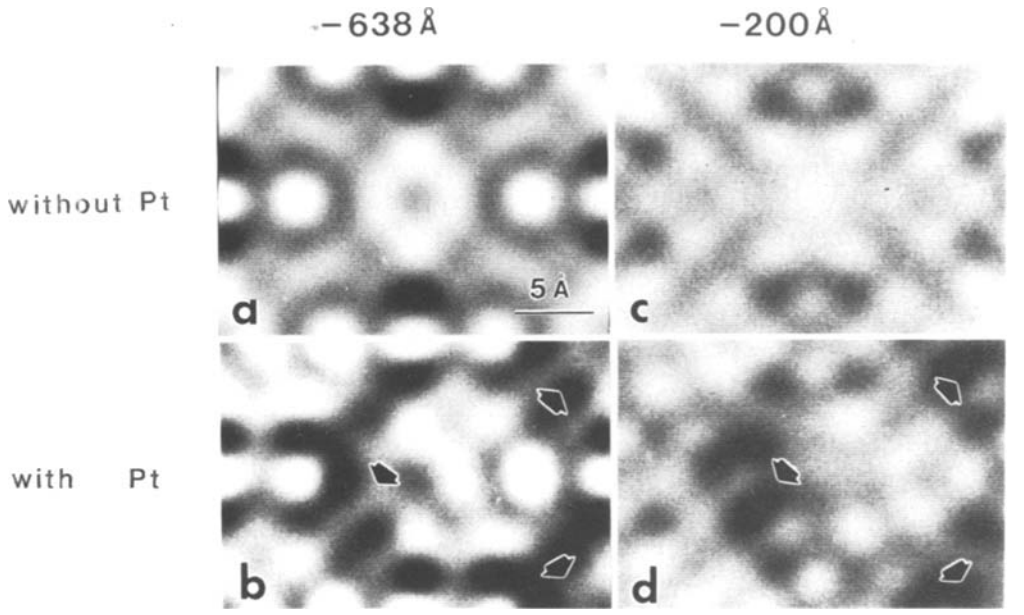

Fig. 5. Simulated HREM images at 200 kV for Y-zeolite in [110] projection. (a), (c) without Pt. (b), (d) with Pt clusters arrowed (55 atoms each). Defocus values are −638 Å for (a) and (b), −200 Å for (c) and (d).

experimental images of fig. 4, but rather to serve as a simple demonstration of the fact that the minimum phase contrast imaging condition is more appropriate than optimum defocus for the detection of small metal clusters inside the zeolite structures. The results of this image simulation are shown in fig. 5 for objective lens defocus values of −200 Å (minimum-phase contrast) and −638 Å (optimum defocus). The arrows in figs. 5b and 5d indicate the centers of the Pt clusters. It is easier to visualize the Pt clusters in fig. 5d than in fig. 5b.

It is highly desirable to be able to locate the positions of Pt clusters inside the zeolites with respect to the zeolite structure. Scanning transmission electron microscopy (STEM) and microdiffraction have proven to be powerful techniques in the study of structural relationships in some supported metal catalysts [19,20]. Application of the STEM techniques to this series of samples has already produced interesting results which would be extremely difficult to obtain by HREM [21].

4. Conclusions

HREM has been used to characterize highly dispersed Pt metal in NaY- and USY-zeolites. For the Pt/NaY sample, coalescence of small Pt clusters was observed to occur under electron beam irradiation. This phenomenon tends to

accompany structural damage of the zeolites. In general the particle size distributions of highly dispersed metals in zeolites determined solely by TEM are very sensitive to experimental conditions, because the zeolites are easily damaged by the electron beam. In order to interpret particle size distribution results of particles smaller than 10 Å, the possibility of electron beam induced sintering must be considered. In fact, the imaging conditions must be similar for proper comparison between particle size distributions in different images. For Pt in USY-zeolites, Pt coalescence was rarely observed under the same HREM imaging conditions as that used in Pt/NaY. In this series of samples small Pt particles generally did not show up in the HREM images recorded at optimum defocus. Minimum phase contrast imaging has proven to be a very effective method for revealing the small Pt clusters.

Due to the strong phase contrast and the electron beam sensitivity of the zeolite support it is extremely difficult to study the structural relationships between the small Pt particles and the zeolite by HREM. Other techniques such as STEM and microdiffraction may prove more effective in solving the problem. Some initial experiments have been carried out. The results of those experiments will be presented in a separate communication at a later date.

Acknowledgements

We thank Drs. P. Labun, R. Sharma for their assistance on JEM-4000EX and David J. Smith for helpful comments. This work was supported by NSF grant DMR-8618282 and made use of the ASU Facility for HREM supported by NSF grant DMR-8611609.

References

[1] E.J. Demmel, A.D. Perrella, W.A. Stover and J.P. Shambaugh, Oil Gas J. 64 (1966) 178.
[2] T.R. Felthouse and J.A. Murphy, J. Catal. 98 (1986) 411.
[3] M. Boudart, M.G. Samant and R. Ryoo, Ultramicroscopy 20 (1986) 125.
[4] D.W. Breck, *Zeolite Molecular Sieves* (Wiley, New York, 1974) pp. 92–97.
[5] I.Y. Chan, R. Csencsits, M.A..O'Keefe and R. Gronsky, J. Catal. 103 (1987) 466.
[6] N.I. Jaeger, P. Ryder and G. Schulz-Ekloff, Stud. Surf. Sci. Catal. 18 (1984) 299.
[7] L.A. Bursill, E.A. Lodge and J.M. Thomas, Nature (London), 286 (1980) 111.
[8] L.A. Bursill, E.A. Lodge and J.M. Thomas, J. Phys. Chem. 85 (1981) 2049.
[9] M. Audier, J.M. Thomas, J. Klinowski, D.A. Jefferson and L.A. Bursill, J. Phys. Chem. 86 (1982) 581.
[10] G.W. Qiao, J. Lu, J. Zhou and K.H. Kuo, J. Catal. 103 (1987) 170.
[11] O. Terasaki, J.M. Thomas and G.R. Millward, Proc. R. Soc. Lond. A395 (1984) 153.
[12] G.R. Millward, S. Ramdas and J.M. Thomas, Proc. R. Soc. Lond. A399 (1985) 57.
[13] M.M.J. Treacy and J.M. Newsam, Ultramicroscopy 23 (1987) 411.
[14] R. Csencsits and R. Gronsky, Ultramicroscopy 23 (1987) 421.

[15] L.A. Bursill, J.M. Thomas and K.J. Rao, Nature (London) 289 (1981) 157.
[16] E.H. Hirsch, Nature (London) 293 (1981) 759.
[17] L. Petrakis, M.A. Springuel-Huet, T. Ito, T.R. Hughes, I.Y. Chan and J. Fraissard, in: *Proc. 9th Intern. Congress on Catalysis*, Calgary (1988) Vol. 2, p. 348.
[18] K. Heinemann and F. Soria, Ultramicroscopy 20 (1986) 1.
[19] M. Pan, J.M. Cowley and I.Y. Chan, J. Appl. Cryst. 20 (1987) 300.
[20] M. Pan, J.M. Cowley and R. Garcia, Micro & Microscopia Acta 18, No. 3 (1987) 165.
[21] M. Pan, J.M. Cowley and I.Y. Chan, Ultramicroscopy, in press.